

Airborne wear particle emission from train brake friction materials with different contents of steel and copper fibres

Yurii Tsybrii^{a,*}, Izabela Zglobicka^b, Michal Kuciej^b, Oleksii Nosko^a, Karol Golak^b

^a Gdansk University of Technology, Faculty of Mechanical Engineering and Ship Technology, ULG. Narutowicza 11/12, Gdansk, 80-233, Poland

^b Białystok University of Technology, Faculty of Mechanical Engineering, Ul. Wiejska 45C, Białystok, 15-351, Poland

ARTICLE INFO

Keywords:

Train brake friction material
Steel fibre
Copper fibre
Wear
Airborne wear particles

ABSTRACT

This study investigated the influence of the amount of steel and copper fibres in a train brake friction material on the tribological performance, emission intensity and characteristics of airborne wear particles. The particles were generated on a pin-on-disc tribometer under controlled friction and environmental conditions. It was found that the steel fibre results in a more intensive emission of 0.3–10 μm particles compared to the copper fibre. The abrasive wear of the steel disc sample is a predominating source of iron in 1–10 μm particles. The content of iron in these particles is proportional to the relative wear of the disc sample, whilst the content of copper increases with that in the friction material.

1. Introduction

Brake wear particles represent a significant source of airborne particulate matter with contribution of up to about 20% of total traffic-related particulate matter (Grigoratos and Martini [1], Padoan and Amato [2], Kukutschová and Filip [3]). Containing toxic content in the form of heavy metals and resins, these particles result in poor air, soil and water quality, affecting the health of people and animals and damaging buildings. With an increasing fleet of cars, buses, trams, trains and other transport vehicles, more and more brake wear particles are emitted to the atmosphere, which is especially noticeable for semi-closed environments like traffic tunnels, public transport stops, train and metro stations. Nowadays many countries, including those of the European Union, make efforts to reduce transport-related particle emissions [4].

Friction materials used in the brakes of transport vehicles contain a number of ingredients which are traditionally classified into the following groups: binders, fillers, reinforcing fibres and friction additives. Copper is commonly used as reinforcing fibres and friction additives that are added to the material formulation in the form of fibres or powders. This metal, possessing high thermal conductivity, intensifies the removal of heat from the friction zone and, thereby, results in a lower contact temperature (Bijwe et al. [5]). By contributing to the formation of primary and secondary contact plateaus (Eriksson and Jacobson [6]), copper fibres allow to improve the tribological

performance, e.g. sustain and stabilise the friction coefficient, decrease the wear, reduce the noise emission (Österle et al. [7], Kumar and Bijwe [8], Tavangar et al. [9]). Nonetheless, copper in brake wear debris can potentially have toxic effects on human health. Therefore, there is a global trend to reduce the amount of copper in the friction materials (Straffellini et al. [10]).

Steel reinforcing fibres represent another common ingredient in the friction material formulation. They improve the strength properties of the friction material (Kumar and Bijwe [11]) and, similarly to copper fibres but not to such extent, promote the heat removal from the friction zone (Bijwe and Kumar [12]). They play also an important role in the formation of primary and secondary contact plateaus modifying the tribological characteristics. Therefore, steel fibres are considered to be a good candidate to partially or fully replace copper in brake friction materials (Jang et al. [13], Leonardi et al. [14], Lee et al. [15], Mahale et al. [16]).

A number of studies have been devoted to the quantification and characterisation of airborne wear particles emitted from brake materials. In most of them, the experimental set-up with the tested friction pair is isolated from the environment by a clean chamber. There are, however, not so many studies focusing on the influence of the amount of steel and copper fibres in the friction material formulation on the emission of airborne wear particles and their physicochemical characteristics. Wahlström et al. [17] investigated the concentration, size distribution and elemental composition of wear particles from car brake

* Corresponding author.

E-mail address: yurii.tsybrii@pg.edu.pl (Y. Tsybrii).

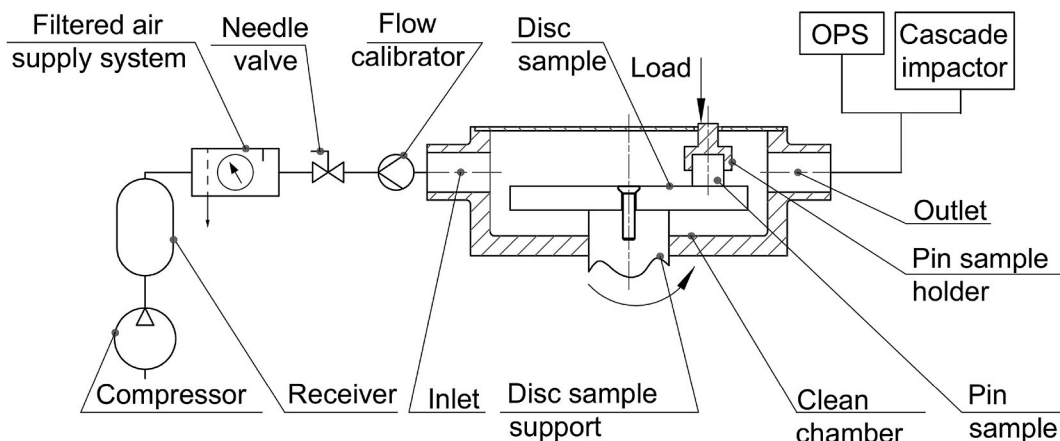


Fig. 1. Schematic of the experimental set-up.

Table 1

Formulations of the friction materials, wt%.

Ingredient	Friction material				
	M0%	MFe16%	MFe30%	MCu18%	MCu32%
Caoutchouc	13.9	12.4	11.2	12.1	10.8
Phenol formaldehyde resin	13.9	12.4	11.2	12.1	10.8
Vulcaniser and hardening agent	1.3	1.2	1	1.1	1
Mineral fibre	18.2	16.3	14.7	15.9	14.1
Graphite	19.9	17.8	16.1	17.4	15.5
Stibnite	3.9	3.4	3.2	3.4	3
Calcium carbonate	28.9	19.9	12.6	19.5	12
Steel fibre		16.6	30		
Copper fibre				18.5	32.8

pads with iron and copper contents using a disc brake test stand. Kukutschová et al. [18] performed a complex chemical and microscopic analysis of the wear particles generated by an automotive brake dynamometer equipped with car brake pads containing iron and copper. Alemani et al. [19] investigated the emission intensity, size distribution and elemental composition of wear particles for several car brake materials with different contents of iron and copper using a pin-on-disc tribometer. Lyu et al. [20] conducted a pin-on-disc study of the friction, wear and wear particle emission characteristics of three materials, a copper-containing reference material and its two copper-free modifications with increased amount of steel fibre. Wei et al. [21] performed a study of the friction and wear behaviour, wear particle emission and brake squeal noise of three materials with copper, steel or ceramic fibre using a pin-on-disc test rig. Gomes Nogueira et al. [22] investigated a copper-free material and its two modifications containing barite or a larger amount of steel fibre using a pin-on-disc tribometer in terms of friction and wear behaviour in relation to the elemental compositions of the bulk material, friction layers and wear particles. Song et al. [23] investigated the effect of the reinforcing fibres made of steel, mineral, cellulose and aramid in a copper-free friction material on the concentration and size distribution of brake wear particles using a Krauss-type tribometer. Wei et al. [24] performed a pin-on-disc study of the tribological performance, wear particle emissions and brake squeal noise of two copper-free brake materials with carbon fibre or carbon nanotubes as the replacement for copper fibre.

The studies mentioned above used basically two types of

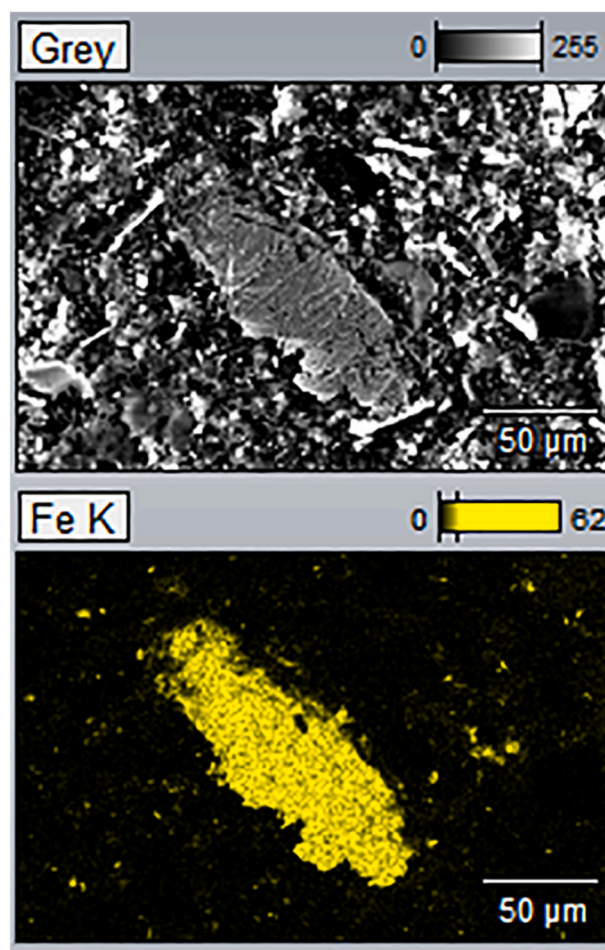


Fig. 2. SEM image of a single steel fibre and EDX map of Fe element.

experimental set-ups, namely, dynamometers and pin-on-disc tribometers. The dynamometer approach allows a better reproduction of the friction conditions in a brake with account of its design. On the other hand, the pin-on-disc approach provides accurate and controllable conditions at the sliding contact, including more uniform distributions

Table 2
Elemental compositions of the samples, wt%.

Element	Pin sample					Disc sample
	M0%	MFe16%	MFe30%	MCu18%	MCu32%	
C	45.5	47.3	32	44	47.2	0.3
O	27.2	20.3	32.7	20.6	20.6	
Mg	0.9	0.7	0.4	0.3	0.3	
Al	2.1	1.3	0.9	0.9	1	
Si	3.8	2.7	2	1.9	1.9	0.1
S	1.8	2.4	1.6	2.4	2.4	
Ca	16.5	12.5	9.1	12.2	8.5	
Cr						1.2
Mn						0.9
Fe	1.7	11.7	21	1.2	0.5	97
Ni						0.2
Cu				16.3	17.3	
Mo						0.2

of the contact pressure and sliding velocity, which is important when studying the mechanisms of wear and airborne wear particle generation.

The present study aimed at the investigation of the influence of steel and copper fibres in the friction material on the tribological performance and emission intensity, morphology, elemental composition of airborne wear particles. Five experimental train brake friction materials with known formulations were tested against steel using a pin-on-disc tribometer with the friction pair isolated from the environment. The main focus of the study was put on analysing the relationship between the wear of the friction pair and wear particle characteristics.

2. Experimental

2.1. Tribological study

Fig. 1 shows a schematic of the experimental set-up based on a T-11 pin-on-disc tribometer. In this tribometer, the pin sample is pressed against the disc sample by a dead weight of maximum 50 N, whilst the disc sample can rotate with a constant speed up to 1000 RPM. The distance between the axes of the pin and disc samples (average friction radius) was set equal to 20 mm. A force transducer HBM S2 measured

the friction force with resolution 0.01 N. A K-type thermocouple measured the temperature T of the pin sample at distance 1 mm from the friction surface. A Radwag XA 210.4Y.A PLUS analytical balance was used to measure the mass wear w_{pin} of the pin sample and mass wear w_{disc} of the disc sample with resolution 0.01 mg.

2.2. Airborne wear particle measurements

The pin-on-disc pair of the tribometer was isolated from the environment by a clean chamber of volume 0.55 L (see Fig. 1). A Bambi PT50D compressor supplied air to the clean chamber inlet through a 50 L receiver and a TSI Filtered Air Supply 3074B system. The inlet airflow was adjusted by a needle valve RFL-B-3/8 and a TSI Flow Calibrator 4048 to the value of 12 L/min. The particles generated at the pin-on-disc contact were carried by the forced airflow inside the clean chamber. The air at the clean chamber outlet was sampled by a TSI Optical Particle Sizer 3330 (OPS) and a Dekati PM10 Cascade Impactor (CI) with respective rates 0.75 L/min and 9.75 L/min.

OPS classifies 0.3–10 μm optical size particles into 16 size fractions by measuring the amount of light scattered by an individual particle passing through a beam of light. The midpoints of the size fractions are 0.337, 0.419, 0.522, 0.65, 0.809, 1.007, 1.254, 1.562, 1.944, 2.421, 3.014, 3.752, 4.672, 5.816, 7.242, 9.016 μm . The particle concentration C_{OPS} measured by OPS is expressed in no/cm^3 . CI is a three-stage cascade impactor with cutpoints 10, 2.5 and 1 μm . It collects particles of inertial size fractions >10 μm , 2.5–10 μm and 1–2.5 μm on aluminium filters for subsequent microscopy and chemical studies.

Before each test, the clean chamber, parts of the tribometer inside the clean chamber, silicon tubes connecting the clean chamber with the inlets of OPS and CI, parts of CI were carefully cleaned. The particle concentration C_{OPS} was checked to be equal to zero in the absence of friction.

2.3. Microscopy and elemental analysis

The original pin samples, worn pin and disc samples and filters of CI with collected wear particles were investigated using field-emission scanning electron microscopy (SEM). For high resolution imaging, the samples were coated with carbon using a Gatan PECS coating system. The observations were carried out by an ultra-high-resolution analytical

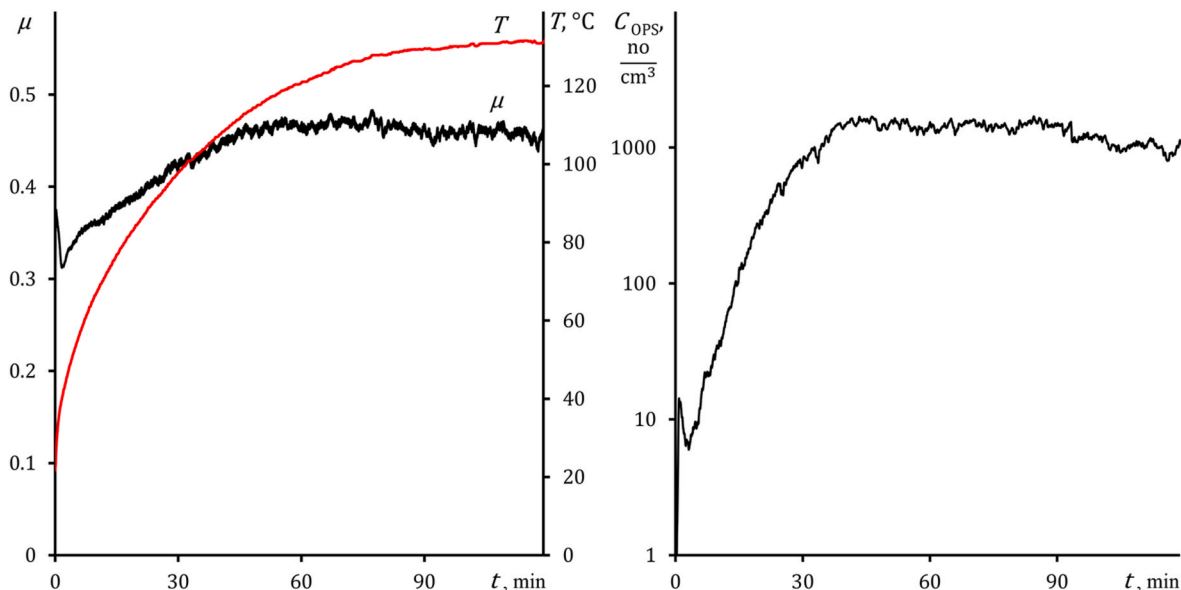


Fig. 3. Typical test results (M0%, 1 MPa \times 1.8 m/s).

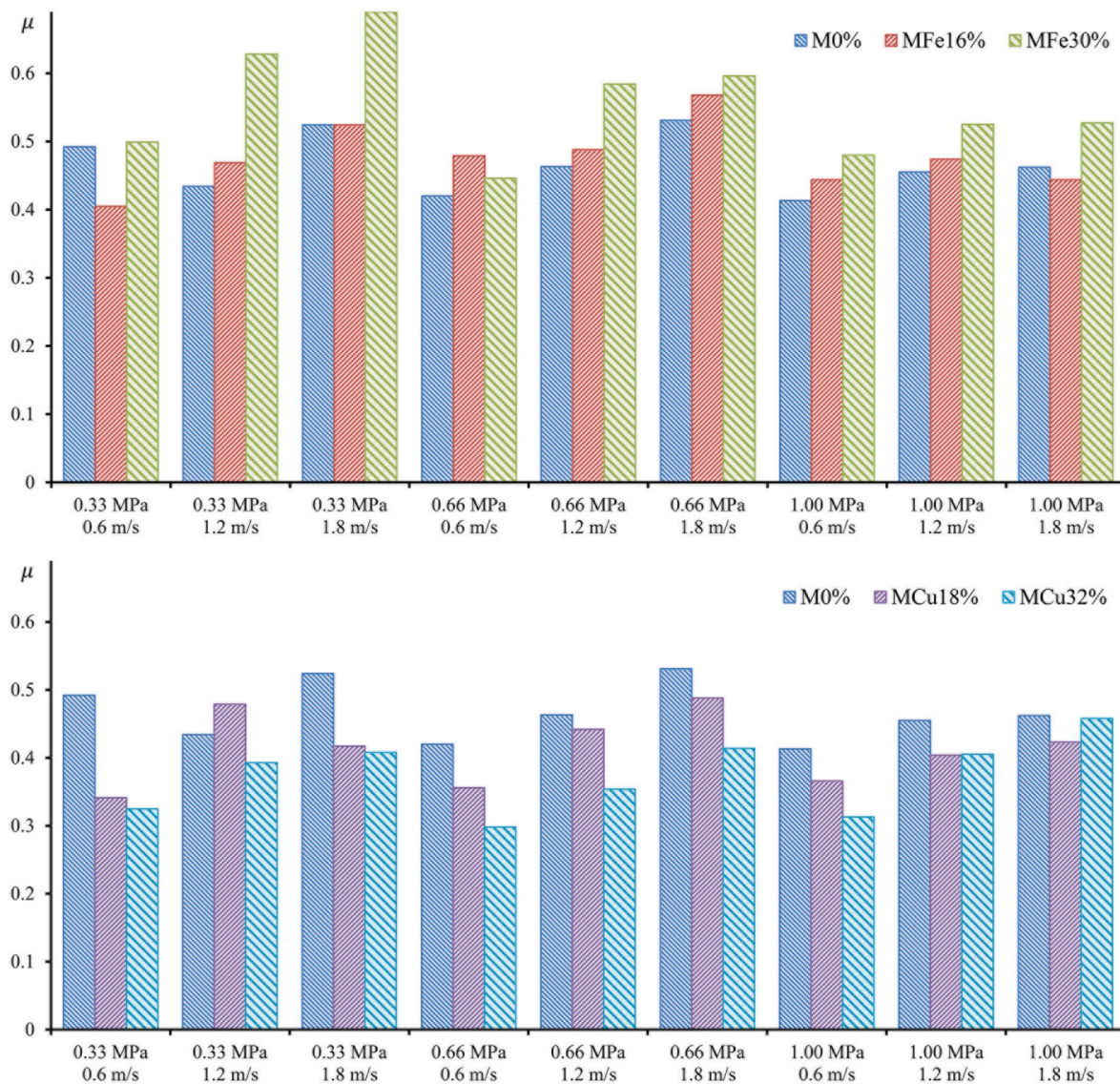


Fig. 4. The friction coefficient μ depending on the friction regime.

Thermo Scientific Scios 2 Dual Beam FIB-SEM system at electron acceleration voltage 2 kV. The magnification varied from 500 to 35 000. The elemental analysis was performed using a NORAN System 7 energy dispersive full range X-ray microanalysis system (EDX) at voltage 20 kV and elemental range 10 kV.

2.4. Friction materials

The friction materials were manufactured according to a full-scale production technology for train brake shoes. Their formulations are presented in Table 1.

M0% is the reference material that has no steel or copper content. MFe16% and MFe30% contain respectively 16.6 wt% and 30 wt% of steel fibre. Fig. 2 shows a microscopic image of a single steel fibre. MCu18% and MCu32% contain respectively 18.5 wt% and 32.8 wt% of copper fibre. Among the mentioned friction materials, the formulation

of MFe30% is the closest to those used for manufacturing commercial brake shoes. The basic stages of the production technology included dry mixing of the ingredients into a mixture, seasoning and milling of the mixture, hot moulding and curing. The pin samples, 8 mm in diameter, were milled out from the manufactured brake shoes on a 6040T4D milling machine. The original friction surface was not altered during the process.

The disc samples, 60 mm in diameter, were cut out from 42CrMo4 steel bars. Table 2 presents the EDX elemental compositions of the pin and disc samples. The friction surface of the disc sample had hardness 180 HB.

2.5. Friction conditions

The friction materials were tested at 3 levels of contact pressure (0.33, 0.66 and 1 MPa) and 3 levels of sliding velocity at the average

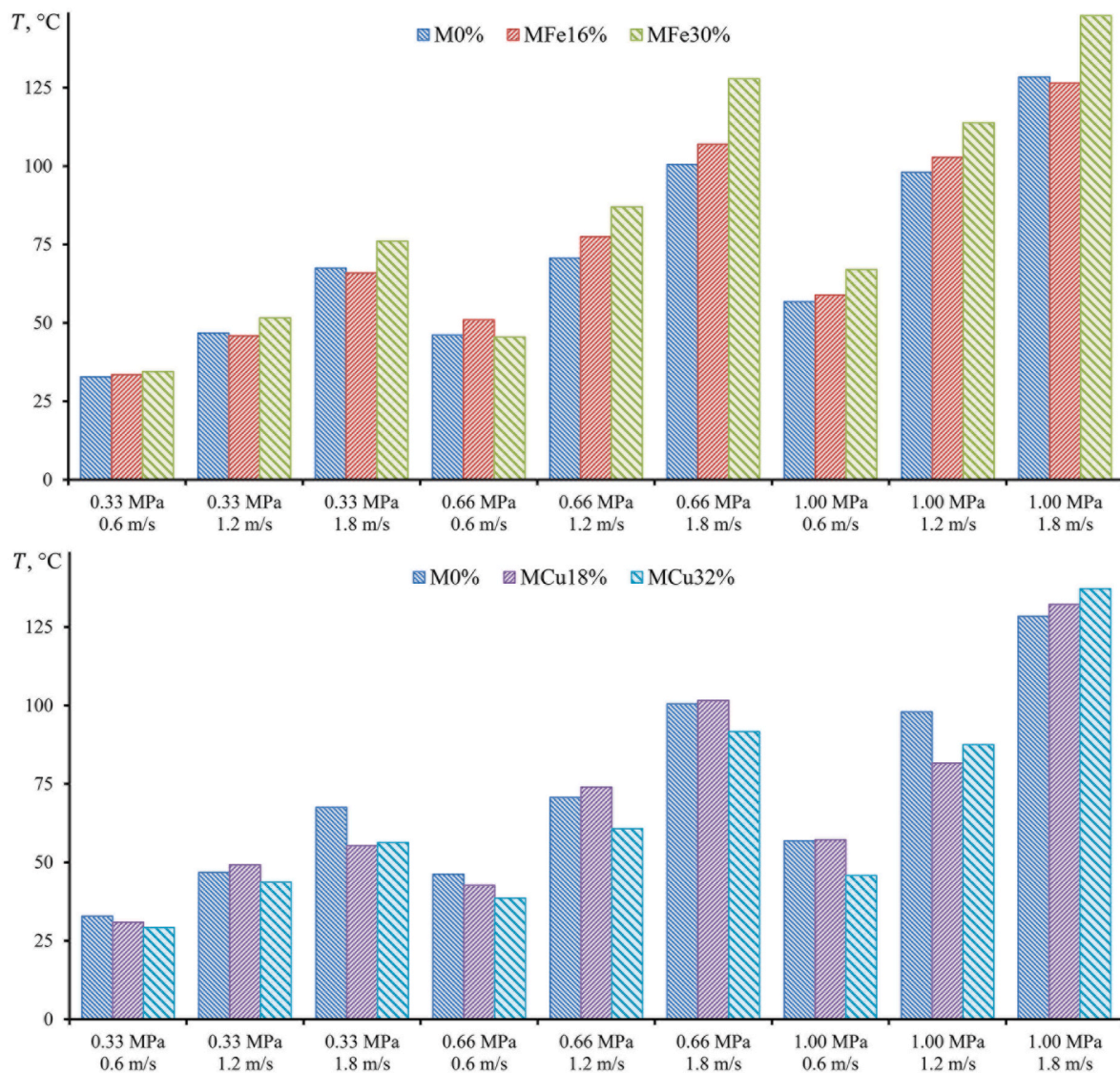


Fig. 5. The pin sample temperature T depending on the friction regime.

friction radius (0.6, 1.2 and 1.8 m/s). Each test was conducted with a new pair of pin and disc samples during 120 min at room temperature 22 ± 2 °C and relative humidity $35 \pm 5\%$. All tests were conducted under similar conditions, including the environmental conditions, equipment settings, experimental procedures and operator.

The typical results from a single test conducted in the heaviest friction regime of $1 \text{ MPa} \times 1.8 \text{ m/s}$ are shown in Fig. 3. Transient frictional and thermal processes take place during the first hour of the test. The behaviour of the investigated characteristics, including μ , T and C_{OPS} , stabilises with time and is close to stationary during the second hour of the test. The present study focusses on their stationary values determined by averaging over the second hour of the test.

It should be mentioned that the contact pressure range of 0.33–1 MPa covers the values set in the in-vehicle experiments (Abbasi et al.

[25]) and full-scale dynamometer experiments (Namgung et al. [26], Zhang et al. [27]). On the other hand, the sliding velocity is low due to the tribometer limitations. Its range of 0.6–1.8 m/s corresponds to the smallest initial values in the sub-scale dynamometer experiments (Wang et al. [28]) and pin-on-disc tribometer experiments (Olofsson [29], Zhang et al. [30]). Accordingly, the temperature T of the pin sample (see Fig. 3) is lower than the temperature of the brake shoe/pad under a real braking scenario that may reach hundreds of degrees Celsius. Thereby, the experimental set-up allows investigating the relationship between the amount of steel and copper fibres in the friction material and the tribological and wear particle characteristics under low velocity and low temperature conditions.

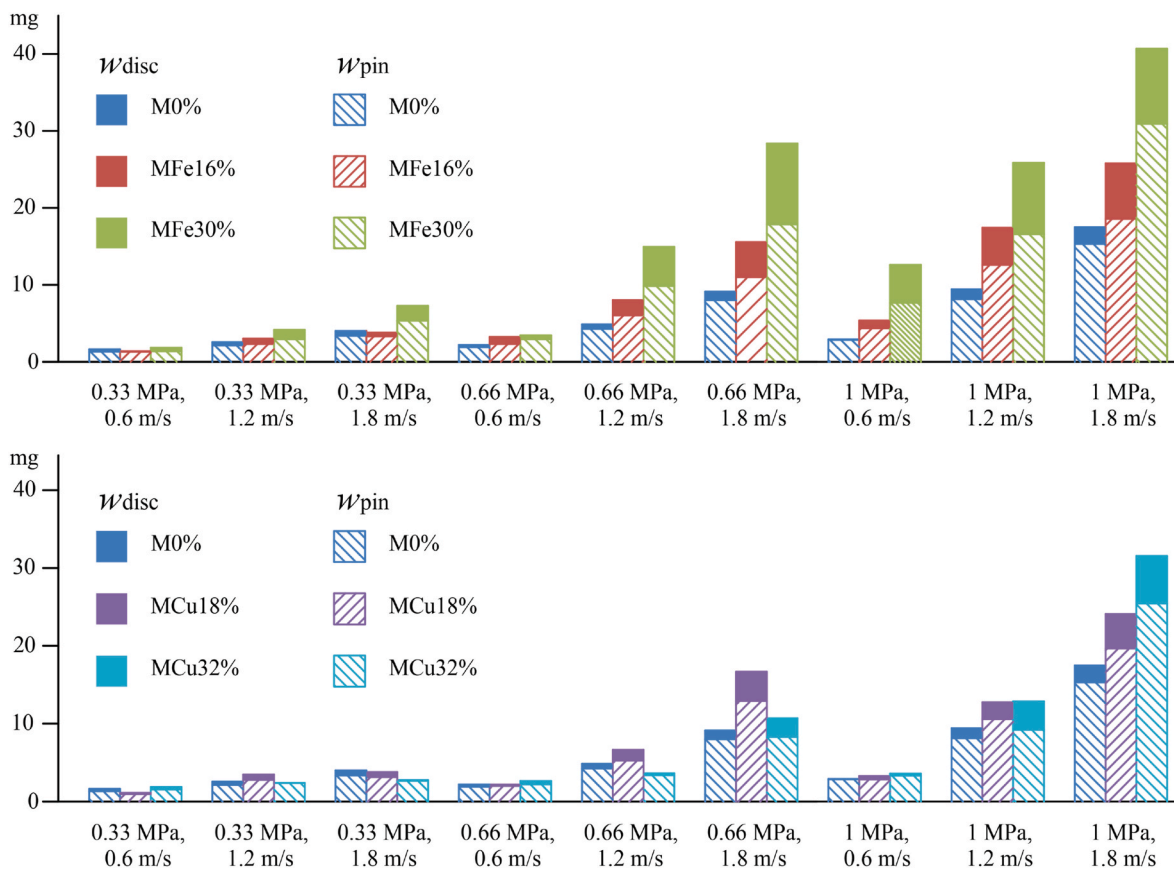


Fig. 6. Pin sample wear w_{pin} and disc sample wear w_{disc} depending on the friction regime.

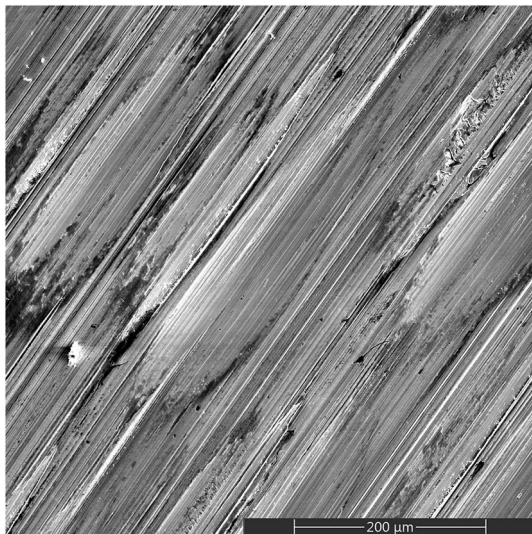


Fig. 7. SEM image of the worn surface of the disc sample (MFe16%, 1 MPa × 1.8 m/s).

3. Results and discussion

3.1. Tribological characteristics

The obtained values of the friction coefficient μ are shown in Fig. 4. For the friction materials and regimes under study, μ varies between 0.3 and 0.7. The test-retest variability of μ is about 7%. It is seen that the addition of steel or copper fibre to the friction material formulation has a noticeable impact on μ . An increase in the content of steel fibre leads to an increase in μ , which is in line with the studies by Bijwe and Kumar [12] and Mahale et al. [16]. On the other hand, an increase in the content of copper generally leads to a decrease in μ . This trend is, however, in contradiction to those discussed next. Kumar and Bijwe [8] and Leonardi et al. [14] found that μ increases with the content of copper in the friction material. Lyu et al. [20] and Wei et al. [21] concluded that μ is comparable for copper-containing and copper-free materials with the same reference formulation. In these studies, the content of copper did not exceed 20 wt% which is considerably lower than that in MCu32%.

Note that the studies mentioned above investigated the friction materials intended for car brakes, with the formulations differing from those used in the present study (see Table 1). Therefore, the corresponding comparisons of the tribological characteristics and trends should be considered as qualitative.

The values of the pin sample temperature T are presented in Fig. 5. It is seen that T is about 30 °C for all materials for the lightest friction

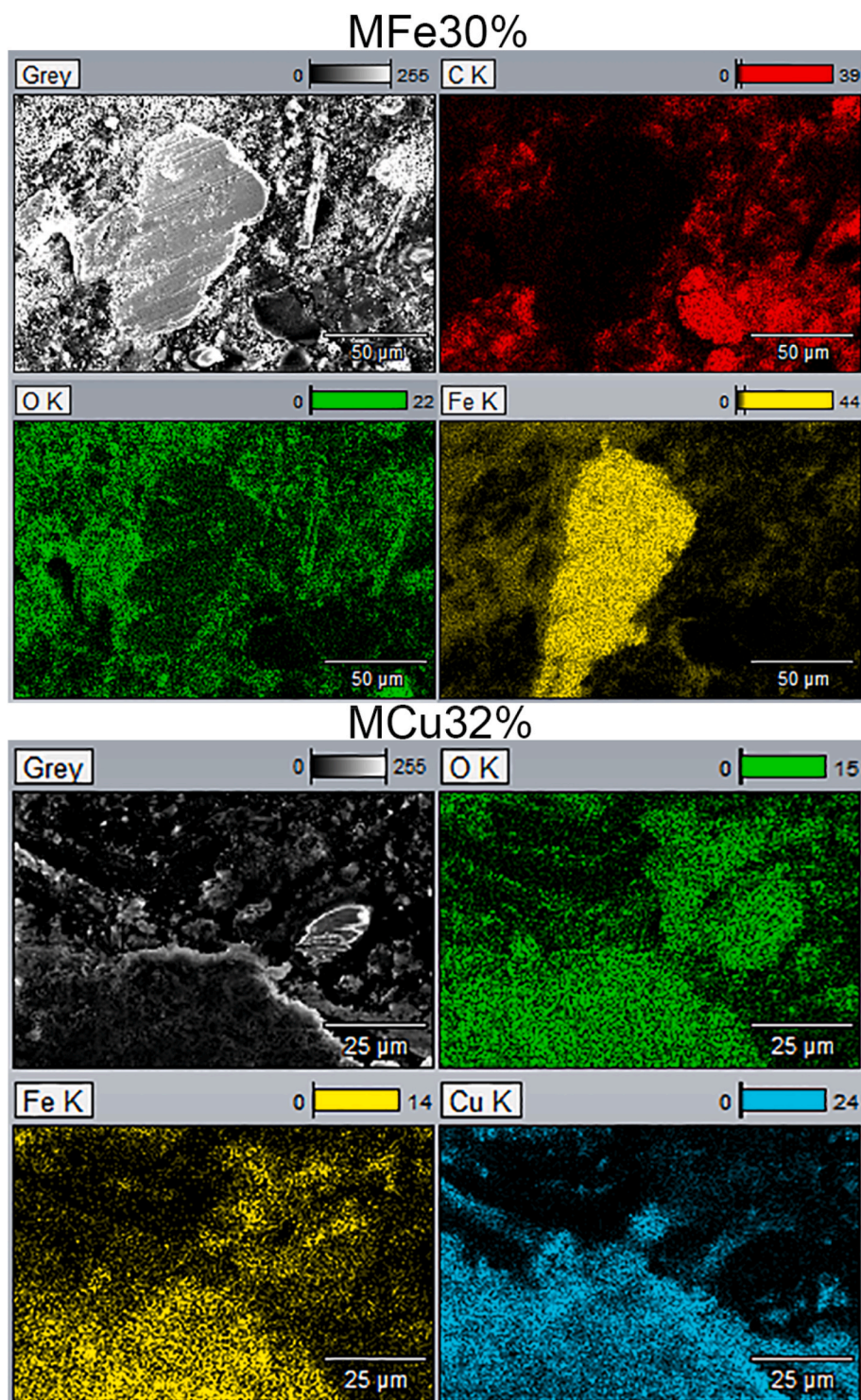


Fig. 8. EDX maps of the worn surfaces of the pin samples (1 MPa \times 1.8 m/s).

regime of 0.33 MPa \times 0.6 m/s. An increase in the contact pressure or sliding velocity results in an increase in T . For the heaviest friction regime of 1 MPa \times 1.8 m/s, T is about 130 °C. The test-retest variability

of T is about 6%.

Fig. 6 presents the experimental data on the pin sample wear w_{pin} and disc sample wear w_{disc} . The test-retest variability of w_{pin} and w_{disc} is

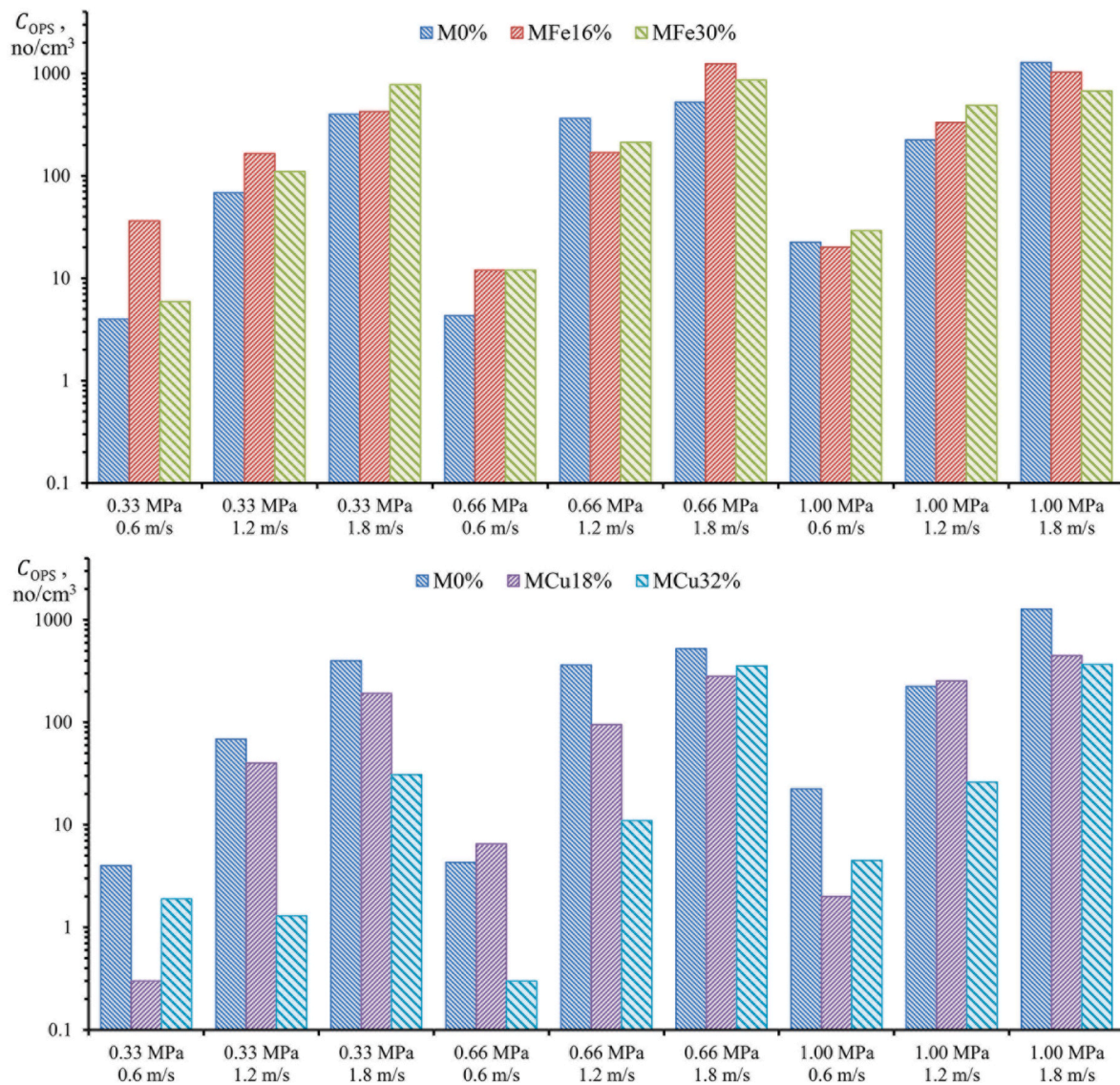


Fig. 9. The particle concentration C_{OPS} depending on the friction regime.

about 15%. As one may expect, both w_{pin} and w_{disc} increase with an increase in the contact pressure or sliding velocity for all materials. An increase in both w_{pin} and w_{disc} is also observed with an increase in the content of steel fibre, especially from MFe16% to MFe30%. The addition of copper fibre generally results in smaller values of w_{pin} and w_{disc} compared to the addition of a similar amount of steel fibre, which agrees well with the results by Jang et al. [13] and Kumar and Bijwe [11]. It is remarkable that an increase in the content of steel or copper fibre leads to a larger value of the relative disc sample wear $w_{disc}/(w_{pin}+w_{disc})$ at the heavier friction regimes.

Fig. 7 shows a typical microscopic image of the worn surface of the disc sample. Numerous ploughing grooves can be seen on the surface, indicating abrasive wear. Fig. 8 presents EDX maps of the worn surfaces of the pin samples with the highest content of steel fibre (MFe30%) and copper fibre (MCu32%). In the case of MFe30%, a primary plateau

dominated by iron is identified along with an adjacent secondary plateau dominated by iron and oxygen. The mentioned above increase in the friction coefficient μ and wear w_{pin} and w_{disc} with an increase in the content of steel fibre is likely attributed to the formation of such plateaus. As regards MCu32%, here a plateau composed mainly of copper, iron and oxygen is identified that may act as a solid lubricant, explaining the mentioned above decrease in μ with an increase in the content of copper (Zhang et al. [27]).

3.2. Particle emission

Fig. 9 shows the values of the particle concentration C_{OPS} . These values are of order 1 to 10³ no/cm³ for all friction materials and regimes. The test-retest variability of C_{OPS} is about 20% for the heavier friction regimes with C_{OPS} of order 10² to 10³ no/cm³ and can be significantly

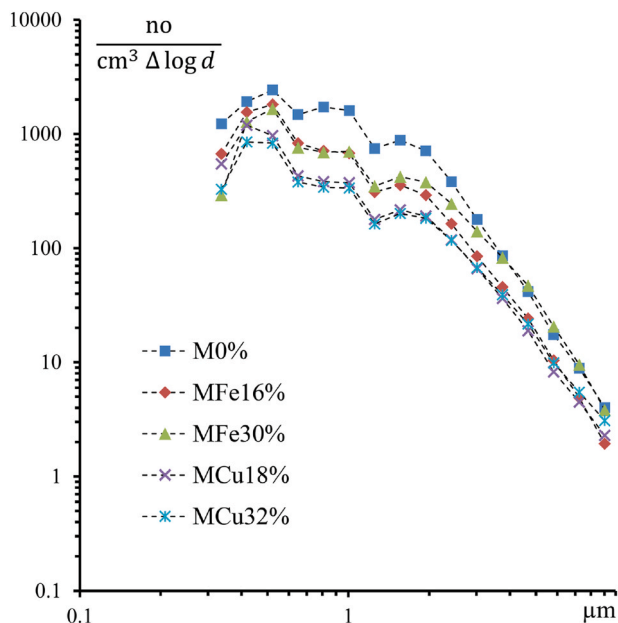


Fig. 10. Particle optical size distributions (1 MPa \times 1.8 m/s).

larger for the lighter friction regimes with C_{OPS} of order 1 to 10^2 no/cm³. No clear dependency can be seen between the content of steel fibre and C_{OPS} . On the other hand, an increase in the content of copper leads to a decrease in C_{OPS} . Comparison of the values of C_{OPS} for the materials containing similar amounts of steel and copper fibres, i.e. MFe16% vs MCu18% and MFe30% vs MCu32%, leads to the conclusion that the steel fibre is responsible for more intensive emission of wear particles. This conclusion is in good agreement with the results obtained by Lyu et al. [20] and Wei et al. [21].

Analysis of the experimental data presented in Figs. 6 and 9 shows that there is practically no correlation between the particle concentration C_{OPS} and wear w_{pin} , w_{disc} , ($w_{pin} + w_{disc}$). This result was previously confirmed for several car brake materials tested under similar friction conditions (Tarasiuk et al. [31]).

Fig. 10 shows the particle size distributions measured by OPS for the heaviest friction regime of 1 MPa \times 1.8 m/s. All presented distributions have a global (within 0.3–10 μ m particle optical size range) peak at about 0.5 μ m and a local peak at about 1.6 μ m. Similar particle size distributions were observed in the studies by Wahlström et al. [17] and Alemani et al. [19]. It is interesting that an increase in the content of steel or copper fibre generally leads to an increase in the fraction of larger particles with optical sizes above 2 μ m. This effect is especially apparent when comparing the distributions for M0% and MFe30%. Wei et al. [21] concluded that the addition of steel fibre to the friction material formulation results in the emission of larger wear particles (in 15–750 nm particle electric mobility size range) compared to the addition of the same amount of copper fibre. The particle size distributions of Fig. 10 give support to this conclusion for 0.3–10 μ m particle optical size range.

3.3. Particle morphology and elemental composition

Airborne wear particles emitted from the pin-on-disc contact were

collected on the filters of CI in the heaviest friction regime of 1 MPa \times 1.8 m/s. Fig. 11 shows the SEM images of the wear particles on 2.5–10 μ m and 1–2.5 μ m particle filters. Particles of various shapes can be noticed for each material, including flaky particles, rounded particles and particle agglomerates. It is remarkable that larger flaky particles correspond to the materials with the highest content of steel fibre (MFe30%) or copper fibre (MCu32%), which correlates with the maximum values of w_{pin} and w_{disc} (see Fig. 6) and above discussed particle size distributions (see Fig. 10).

The emission of large flaky particles with sharp edges and irregular shape suggests abrasive processes at the sliding contact (Kukutschová and Filip [3]), which is supported by the presence of the ploughing grooves in Fig. 7. The agglomerates built up from micrometre-order rounded particles most probably originated from adhesive processes (Olofsson [29], Xiao et al. [32]). Thereby, the mentioned observations identify the wear mechanism as the combination of abrasive and adhesive wear.

Fig. 12 shows the contents of iron and copper in the friction material and corresponding wear particles obtained by EDX. According to these data, the wear particles contain up to about 50 wt% of iron. The amount of iron in 2.5–10 μ m and 1–2.5 μ m inertial size particles is almost the same. Moreover, the friction pairs with the steel fibre free materials (M0%, MCu18%, MCu32%) emit particles containing 25–35 wt% of iron, suggesting that the wear of the disc sample is a predominating source of iron in the airborne wear particles. This result was confirmed in the previous studies, e.g. by Alemani et al. [19] and Gomes Nogueira et al. [22]. As regards the content of copper, it is expectedly present in the wear particles emitted from the pairs with copper-containing materials (MCu18%, MCu32%).

If the disc sample contains 97 wt% of iron (see Table 2), whilst the pin sample contains from 0 to 30 wt% of iron (see Table 1), one can hypothesise that the larger is the contribution of the disc sample wear w_{disc} to the sum wear ($w_{pin} + w_{disc}$) of the friction pair, the higher is the content of iron in the wear particles. Fig. 13 shows the correlation between the relative disc sample wear $w_{disc}/(w_{pin} + w_{disc})$ and content of iron in the wear particles (Fe wt%). A proportional relationship is revealed between these quantities for the wear particles of both inertial size fractions 2.5–10 μ m and 1–2.5 μ m, which supports the mentioned hypothesis.

Fig. 14 presents the correlation between the content of copper in the friction material (see Table 1) and that in the wear particles. It is seen that the content of copper in the wear particles increases with the content of copper in the friction material. Moreover, the relationship is close to proportional for 1–2.5 μ m inertial size wear particles.

It is noteworthy that the results obtained in the present study correspond to the mild friction conditions with the sliding velocity not exceeding 1.8 m/s and pin sample temperature below 160 °C and, therefore, they should be considered as indicative trends. A further study is needed here to investigate the tribological and wear particle emission behaviour of the friction materials depending on the contents of steel and copper fibres under more severe friction conditions that correspond to the operation of train brakes.

4. Conclusion

The present study investigated the influence of the amount of steel and copper fibres in the friction material developed for train brakes on the interrelated tribological characteristics and emission intensity, size distribution, morphology, elemental composition of airborne wear particles. The particles were generated by a pin-on-disc tribometer with

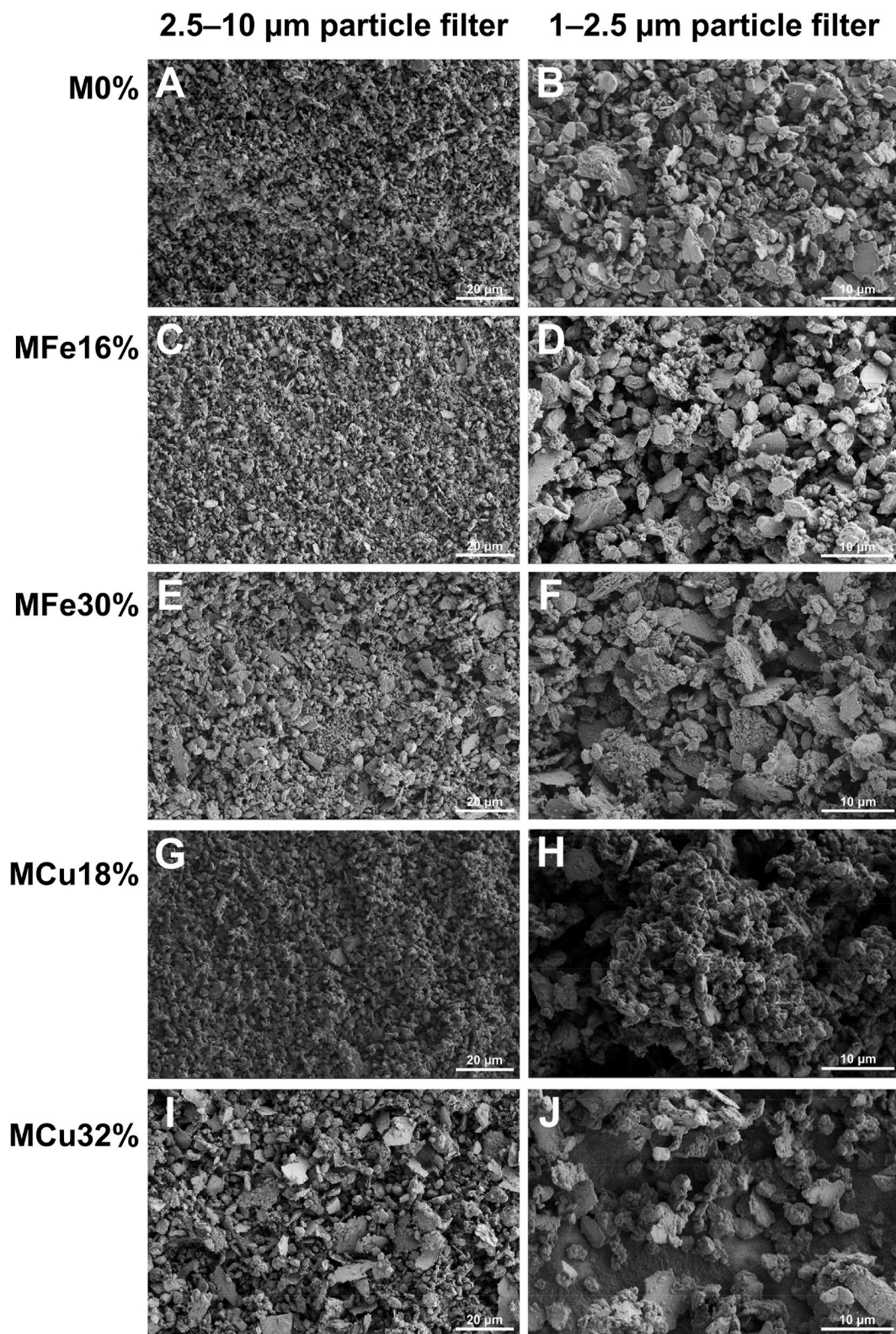


Fig. 11. SEM images of the wear particles (1 MPa \times 1.8 m/s).

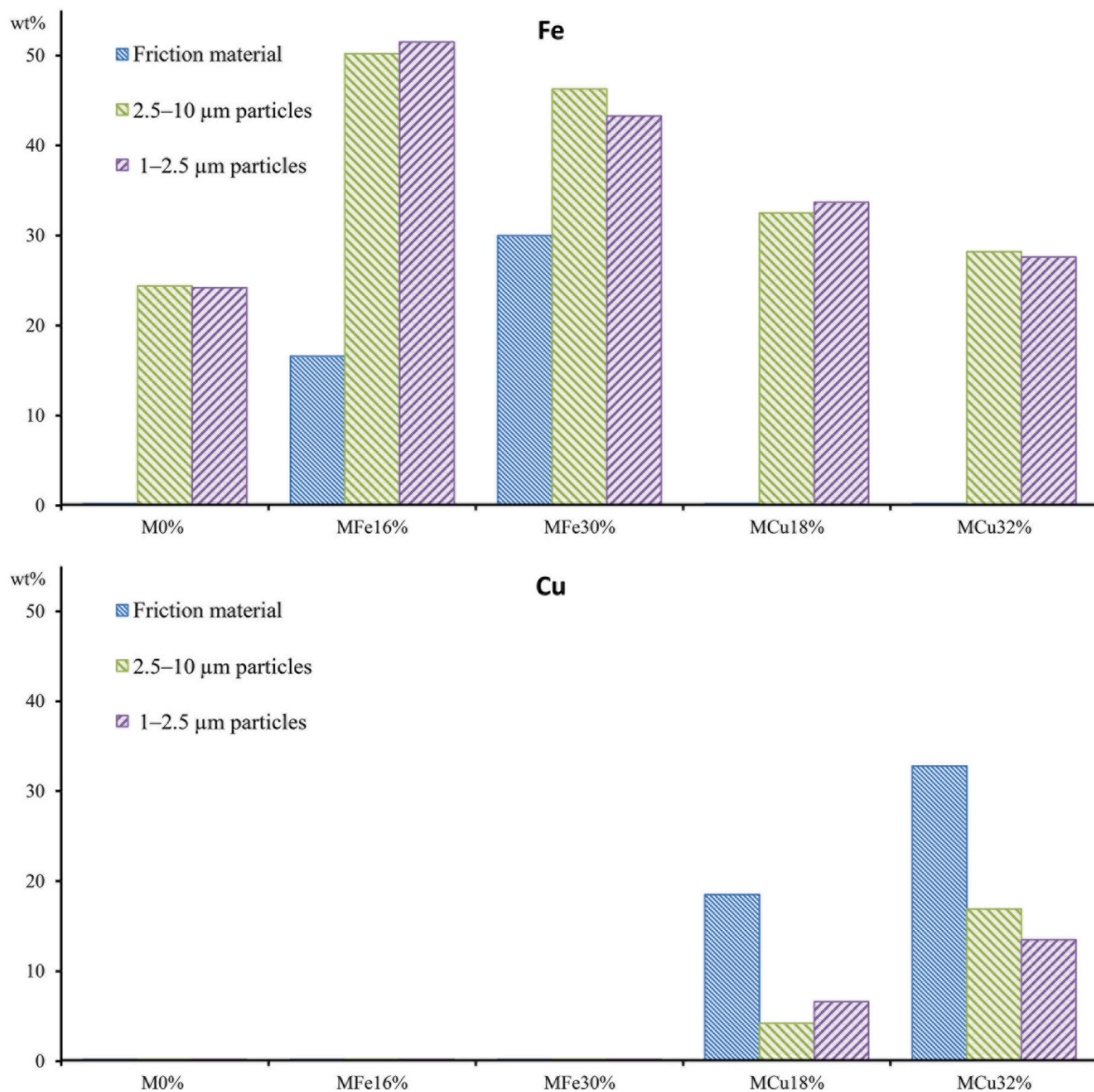


Fig. 12. Contents of iron and copper in the friction material and wear particles (1 MPa × 1.8 m/s).

the friction pair placed inside a clean chamber under controlled friction and environmental conditions. The main findings of the study can be summarised as follows:

- An increase in the content of steel or copper fibre in the friction material (pin sample) leads to a larger relative wear $w_{disc}/(w_{pin} + w_{disc})$ of the disc sample at the heavier friction regimes.
- The addition of steel fibre to the friction material formulation results in a more intensive emission of 0.3–10 μm optical size wear particles than the addition of a similar amount of copper fibre.
- An increase in the content of steel or copper fibre in the friction material leads to an increase in the fraction of above 2 μm optical size particles.
- The abrasive wear of the steel disc sample is a predominating source of iron in 1–10 μm inertial size wear particles. The content of iron in these particles is proportional to the relative disc sample wear $w_{disc}/(w_{pin} + w_{disc})$.
- The content of copper in 1–10 μm inertial size wear particles increases with the content of copper in the friction material.

Funding

The present work was supported by the National Science Centre, Poland [grant number 2017/27/B/ST8/01249].

Credit authorship contribution statement

Yurii Tsybrii: Methodology, Investigation, Validation, Writing - review & editing; Izabela Zglobicka: Methodology, Investigation, Visualization, Writing - review & editing; Michal Kuciej: Funding acquisition, Supervision, Resources, Writing - review & editing; Oleksii Nosko: Supervision, Conceptualization, Formal analysis, Writing - original draft; Karol Golak: Methodology, Resources, Software, Writing - review & editing.

Declaration of competing interest

The authors declare that they have no known competing financial interests or personal relationships that could have appeared to influence the work reported in this paper.

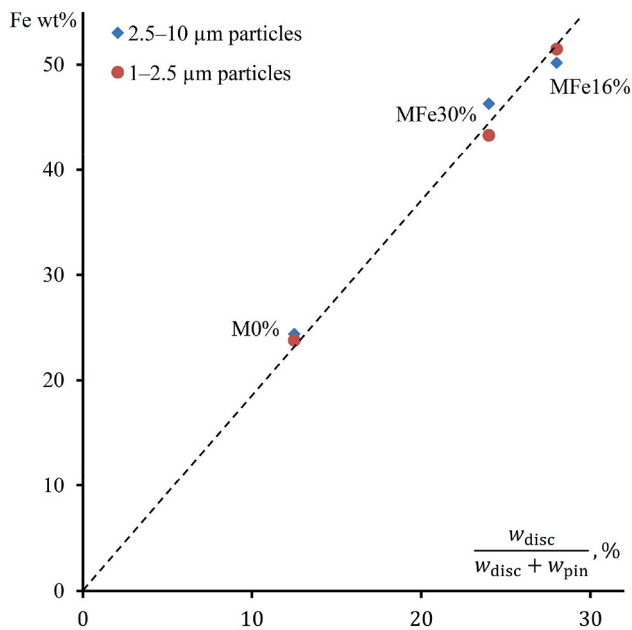


Fig. 13. Correlation between the relative disc sample wear $w_{disc}/(w_{pin} + w_{disc})$ and content of iron in the wear particles (Fe wt%).

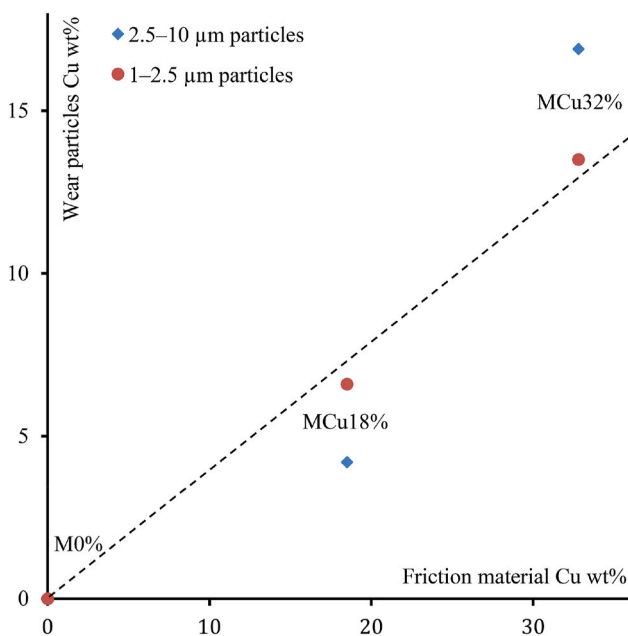


Fig. 14. Correlation between the contents of copper in the friction material and wear particles.

References

- [1] T. Grigoratos, G. Martini, Brake wear particle emissions: a review, *Environ. Sci. Pollut. Control Ser.* 22 (4) (2015) 2491–2504, <https://doi.org/10.1007/s11356-014-3696-8>.
- [2] E. Padoan, F. Amato, Vehicle non-exhaust emissions: impact on air quality, in: F. Amato (Ed.), *Non-exhaust Emissions*, Academic Press, 2018, pp. 21–65, <https://doi.org/10.1016/B978-0-12-811770-5.00002-9>.
- [3] J. Kukutschová, P. Filip, Review of brake wear emissions: a review of brake emission measurement studies: identification of gaps and future needs, in: F. Amato (Ed.), *Non-exhaust Emissions*, Academic Press, 2018, pp. 123–146, <https://doi.org/10.1016/B978-0-12-811770-5.00006-6>.
- [4] *Air Quality in Europe — 2020 Report*, European Environment Agency, 2020 no. 09/2020.
- [5] J. Bijwe, M. Kumar, P.V. Gurunath, Y. Desplanques, G. Degallaix, Optimization of brass contents for best combination of tribo-performance and thermal conductivity of non-asbestos organic (NAO) friction composites, *Wear* 265 (2008) 699–712, <https://doi.org/10.1016/j.wear.2007.12.016>.
- [6] M. Eriksson, S. Jacobson, Tribological surfaces of organic brake pads, *Tribol. Int.* 33 (2000) 817–827, [https://doi.org/10.1016/S0301-679X\(00\)00127-4](https://doi.org/10.1016/S0301-679X(00)00127-4).
- [7] W. Österle, C. Prietzel, H. Kloß, A.I. Dmitriev, On the role of copper in brake friction materials, *Tribol. Int.* 43 (2010) 2317–2326, <https://doi.org/10.1016/j.triboint.2010.08.005>.
- [8] M. Kumar, J. Bijwe, Non-asbestos organic friction composites: role of copper; its shape and amount, *Wear* 270 (2011) 269–280, <https://doi.org/10.1016/j.wear.2010.10.068>.
- [9] R. Tavangar, H.A. Moghadam, A. Khavandi, S. Banaeifar, Comparison of dry sliding behavior and wear mechanism of low metallic and copper-free brake pads, *Tribol. Int.* 151 (2020), 106416, <https://doi.org/10.1016/j.triboint.2020.106416>.
- [10] G. Straffellini, R. Ciudin, A. Ciotti, S. Gialanella, Present knowledge and perspectives on the role of copper in brake materials and related environmental issues: a critical assessment, *Environ. Pollut.* 207 (2015) 211–219, <https://doi.org/10.1016/j.envpol.2015.09.024>.
- [11] M. Kumar, J. Bijwe, Optimized selection of metallic fillers for best combination of performance properties of friction materials: a comprehensive study, *Wear* 303 (2013) 569–583, <https://doi.org/10.1016/j.wear.2013.03.053>.
- [12] J. Bijwe, M. Kumar, Optimization of steel wool contents in non-asbestos organic (NAO) friction composites for best combination of thermal conductivity and tribo-performance, *Wear* 263 (2007) 1243–1248, <https://doi.org/10.1016/j.wear.2007.01.125>.
- [13] H. Jang, K. Ko, S.J. Kim, R.H. Basch, J.W. Fash, The effect of metal fibers on the friction performance of automotive brake friction materials, *Wear* 256 (2004) 406–414, [https://doi.org/10.1016/S0043-1648\(03\)00445-9](https://doi.org/10.1016/S0043-1648(03)00445-9).
- [14] M. Leonardi, C. Menapace, V. Matejka, S. Gialanella, G. Straffellini, Pin-on-disc investigation on copper-free friction materials sliding against cast iron, *Tribol. Int.* 119 (2018) 73–81, <https://doi.org/10.1016/j.triboint.2017.10.037>.
- [15] J.J. Lee, J.A. Lee, S. Kwon, J.J. Kim, Effect of different reinforcement materials on the formation of secondary plateaus and friction properties in friction materials for automobiles, *Tribol. Int.* 120 (2018) 70–79, <https://doi.org/10.1016/j.triboint.2017.12.020>.
- [16] V. Mahale, J. Bijwe, S. Sinha, A step towards replacing copper in brake-pads by using stainless steel swarf, *Wear* (2019) 133–142, <https://doi.org/10.1016/j.wear.2019.02.019>, 424–425.
- [17] J. Wahlström, L. Olander, U. Olofsson, Size, shape, and elemental composition of airborne wear particles from disc brake materials, *Tribol. Lett.* 38 (2010) 15–24, <https://doi.org/10.1007/s11249-009-9564-x>.
- [18] J. Kukutschová, P. Moravec, V. Tomásek, V. Matejka, J. Smolik, J. Schwarz, P. Filip, On airborne nano/micro-sized wear particles released from low-metallic automotive brakes, *Environ. Pollut.* 159 (2011) 998–1006, <https://doi.org/10.1016/j.envpol.2010.11.036>.
- [19] M. Alemani, O. Nosko, I. Metinoz, U. Olofsson, A study on emission of airborne wear particles from car brake friction pairs, *SAE International Journal of Materials and Manufacturing* 9 (2016) 147–157, <https://doi.org/10.4271/2015-01-2665>.
- [20] Y. Lyu, M. Leonardi, J. Wahlström, S. Gialanella, U. Olofsson, Friction, wear and airborne particle emission from Cu-free brake materials, *Tribol. Int.* 141 (2020), 105959, <https://doi.org/10.1016/j.triboint.2019.105959>.
- [21] L. Wei, Y.S. Choy, C.S. Cheung, D. Jin, Tribology performance, airborne particle emissions and brake squeal noise of copper-free friction materials, *Wear* 448–449 (2020), 203215, <https://doi.org/10.1016/j.wear.2020.203215>.
- [22] A.P. Gomes Nogueira, D. Carlevaris, C. Menapace, G. Straffellini, Tribological and emission behavior of novel friction materials, *Atmosphere* 11 (2020) 1050, <https://doi.org/10.3390/atmos11101050>.
- [23] W. Song, J. Park, J. Choi, J.J. Lee, H. Jang, Effects of reinforcing fibers on airborne particle emissions from brake pads, *Wear* (2021), 203996, <https://doi.org/10.1016/j.wear.2021.203996>, 484–485.
- [24] L. Wei, Y.S. Choy, C.S. Cheung, H.K. Chu, Comparison of tribology performance, particle emissions and brake squeal noise between Cu-containing and Cu-free brake materials, *Wear* (2021), 203577, <https://doi.org/10.1016/j.wear.2020.203577>, 466–467.
- [25] S. Abbasi, L. Olander, U. Olofsson, C. Larsson, A. Jansson, U. Sellgren, A field test study of airborne wear particles from a running regional train, *Journal of Rail and Rapid Transit* 226 (2012) 95–109, <https://doi.org/10.1177/0954409711408774>.
- [26] H.G. Namgung, J.B. Kim, M.S. Kim, M. Kim, S. Park, S.H. Woo, G.N. Bae, D. Park, S. B. Kwon, Size distribution analysis of airborne wear particles released by subway brake system, *Wear* 372–373 (2017) 169–176, <https://doi.org/10.1016/j.wear.2016.12.026>.

- [27] P. Zhang, L. Zhang, K. Fu, P. Wu, J. Cao, C. Shijia, X. Qu, Fade behaviour of copper-based brake pad during cyclic emergency braking at high speed and overload condition, *Wear* (2019) 10–23, <https://doi.org/10.1016/j.wear.2019.01.126>, 428–429.
- [28] W.J. Wang, F. Wang, K.K. Gu, H.H. Ding, H.Y. Wang, J. Guo, Q.Y. Liu, M.H. Zhu, Investigation on braking tribological properties of metro brake shoe materials, *Wear* 330–331 (2015) 498–506, <https://doi.org/10.1016/j.wear.2015.01.057>.
- [29] U. Olofsson, A study of airborne wear particles generated from the train traffic — block braking simulation in a pin-on-disc machine, *Wear* 271 (2011) 86–91, <https://doi.org/10.1016/j.wear.2010.10.016>.
- [30] P. Zhang, L. Zhang, D. Wei, P. Wu, J. Cao, C. Shijia, X. Qu, A high-performance copper-based brake pad for high-speed railway trains and its surface substance evolution and wear mechanism at high temperature, *Wear* (2020), 203182, <https://doi.org/10.1016/j.wear.2019.203182>, 444–445.
- [31] W. Tarasiuk, K. Golak, Y. Tsybrii, O. Nosko, Correlations between the wear of car brake friction materials and airborne wear particle emissions, *Wear* (2020), 203361, <https://doi.org/10.1016/j.wear.2020.203361>, 456–457.
- [32] Y. Xiao, Y. Cheng, H. Zhou, W. Liang, M. Shen, P. Yao, H. Zhao, G. Xiong, Evolution of contact surface characteristics and tribological properties of a copper-based sintered material during high-energy braking, *Wear* (2022), 204163, <https://doi.org/10.1016/j.wear.2021.204163>, 488–489.